Supporting Information

AlphaSpace: Fragment-Centric Topographical Mapping to Target Protein-Protein Interaction Interfaces

*David Rooklin[1], Cheng Wang[1], Joseph Katigbak[1], Paramjit S. Arora[1], and Yingkai Zhang[1,2,]**

[1]Department of Chemistry, New York University, New York, New York 10003

[2]NYU-ECNU Center for Computational Chemistry at NYU Shanghai, Shanghai 200062, China

*To whom correspondence should be addressed.

E-mail: yingkai.zhang@nyu.edu

Table of Contents

Implementation and parameterization details

Section S1. Alpha sphere filtration

For the "alpha-atom" model to be accurate, we only consider alpha spheres having radii within a limited range. If an alpha sphere radius is too small, it will represent a position that is not solvent-accessible. Fig. S2C depicts schematically that, in order to accommodate a typical solvent probe (1.4 Å radius), the space must be represented by an alpha sphere with a minimum radius of 3.2 Å. While a non-polar ligand atom (approx. 1.8 Å radius) at this alpha-center would experience some steric overlap with the surface in this minimum radius case, we opt to include these tight but solvent-accessible spaces and hold the minimum alpha sphere radius at 3.2 Å. This is compared to the 3.0 Å minimum implemented by default in fpocket, which can result in the mapping of inaccessible space as in Fig. S1D, where a pocket identified at the interface of Bcl-xL/Bak penetrates into a narrow channel that traverses the interior of the protein. While this solvent-inaccessible channel is an interesting structural feature, it is not meaningful as a fragment-centric binding pocket.

If an alpha sphere radius is too large, the use of its center as an atomic position conferring surface contact becomes less accurate. Conversely, if the maximum radius cutoff drops too far, we will sacrifice the representation of particularly broad pocket structure from the surface map. We use a 5.4 Å maximum radius cutoff to balance between alpha sphere proximity to the surface and the complete representation of concave pocket structure, see Fig. 2B to visualize a geometric model for the relationship between an alpha sphere with the maximum radius and the protein surface. For comparison, the default maximum radius implemented in fpocket is 6.0 Å.

Section S2. Alpha sphere clustering

The goal of our model is to generate a fragment-centric mapping. Since we consider amino acid side chains to be the natural binding fragments in PPIs, we fit this clustering parameter to yield, on average, one alpha-cluster for every side chain engaged in a PPI. We used the complete set of PPI complexes from the 2P2I database,[1,2] listed in Table S1, to perform this parameterization. 2P2I includes a total of 14 PPIs for which orthosteric inhibitors have been developed and for which apo, PPI complex, and iPPI complex structures have been experimentally solved. In the fitting, we are performing topographical mapping on the surface from each PPI that is also targeted by a small-molecule inhibitor. An alpha-cluster, or pocket, is considered to be "occupied" if at least one atom from the peptide or inhibitor is within 1.6 Å of any alpha sphere center from that pocket. Number of side chains per pocket is calculated by dividing the number of side chains in contact with a pocket by the number of pockets in contact with a side chain (omitting pockets exclusively occupied by backbone atoms). As shown in Fig. S4A, the average number of side chains per pocket is near unity when the maximum average-linkage distance is within the range 4.6 to 4.8 Å. For the results in this paper we set this parameter to be 4.7 Å, however this is not intended to be a definitive assignment. Small variation will not significantly impact the overall clustering, but may allow the user to selectively merge or split certain pockets near the cutoff to customize an analysis. For example, for the Mdm2/p53 structure in this paper, we used 4.6 Å in order to separate pockets 6 and 10 to facilitate comparison to the apo and iPPI structures in which these pockets are slightly more distinct (see Fig. 5).

In our filtration strategy, we treat each alpha sphere in an alpha-cluster as an alpha-atom—a theoretical ligand atom with a 1.8 Å radius in approximate contact with the surface. The outline of this set of overlapping alpha-atoms defines the approximate shape of a ligand fragment with structural complementarity to that local interaction space. The enclosed volume of this alpha-cluster pseudo-fragment will represent the approximate volume of an expected fragment binder. Fig. S4B shows the average volumes and standard deviations for all alpha-clusters across the full surfaces of the 14 2P2I proteins, as well as for the subset of clusters located directly at the 14 corresponding PPI interfaces, as a function of the average linkage maximum distance. The average volume is fairly robust with respect to this parameter, and the large standard deviations highlight the sensitivity of our model to capture a large variation in natural modularity from a single average-linkage clustering. To make a general comparison, the average VdW volume for the 20 natural amino acids is 109.2 $Å^3$,[3] which falls in between the full surface and the interface only averages for alpha-cluster volume when using a maximum average linkage distance of 4.7 Å. This comparison indicates that our clusters are in the appropriate range for a fragment-centric model, where a single pocket is to accommodate, roughly, a single side chain. Fig. S4C shows the overlapping histograms for the full surface sets of volumes, the interface only sets of volumes, and the set of volumes for the 20 natural amino acids.

Section S3. Alpha-cluster selection

After all pockets across a protein surface have been identified, the FCTM needs to focus the pocket analysis onto the PPI/iPPI interface. This focus can be restricted to include only pockets in direct contact with the peptide or inhibitor binding partner, or it can be broadened to also include unoccupied pockets in the local vicinity of the interface. AlphaSpace provides two approaches to perform this selection. The first option detects an interface pocket if there is direct contact between at least one alpha sphere and an atom from the peptide or inhibitor binder, using a 1.6 Å contact distance cutoff. This is the set of contact pockets. Adjacent unoccupied pockets can be identified by searching for overlap between the atom list of an unoccupied pocket and the atom list of the contact pockets, and interface expansion is tuned by a threshold ratio of contact pocket atoms required in the unoccupied pocket list. The second option involves the use of an interface atom list, which is calculated using Naccess[4] and is defined to include any atom with SASA occluded by the presence of the peptide or inhibitor binder at the interface. For this approach, a minimum fraction of a pocket's atoms must be found in the interface atom list in order to qualify as an interface pocket. The value of this parameter controls the scale of the interface expansion. For example, the three unoccupied pocket at the Mdm2/p53 interface, depicted in Fig. 5A, are detected when the minimum fraction of interface atoms is set to 50%. The sum set of contact pocket atoms or the interface atom list from a PPI can alternatively be applied to the mapping of the similar apo protein in order to focus the FCTM to the same surface region.

An alternative mode of pocket selection will screen pocket by feature, in order to, for example, include only high-scoring pockets. While AlphaSpace also provides this useful functionality, we emphasize that a complete interaction analysis requires a complete interface map. In fpocket, all pockets containing fewer than 35 alpha spheres are screened out by default. From a cavity-centric perspective, pockets smaller than this might be considered insignificant, however, from a fragment-centric perspective, this results in an aggressive pruning of meaningful pockets (see the comparatively sparse interface coverage for the fpocket results in Fig. S1C and S1D). In fact, we have identified cases where

even diminutive pockets defined by one or two alpha spheres appear to express functional fragment-centric modularity. Fig. S10 highlights one and two alpha sphere pockets engaged in specific fragment-centric interactions at the Xiap-Bir3/Caspase-9 interface. By default, AlphaSpace does not screen alpha-clusters by number of alpha spheres.

Section S4. Pocket ranking

A practical pocket-score should reflect a maximal affinity model, where the score is proportional to the affinity we can expect to achieve between each pocket and a hypothetical complementary inhibitor fragment. Previously, Huang et al. demonstrated that the small-molecule druggability of classical targets could be accurately predicted using a simple biophysical model based on 2 features alone: non-polar surface area and pocket curvature.[5] From observation, we hypothesized that, as a single term, the total alpha-space of a fragment-centric pocket seemed to reflect both the surface area (SA) as well as the curvature associated with that interaction region. To test our hypothesis, we established our own SA and curvature-based metrics, inspired by Huang's model, and evaluated their correlation with total alpha-space. We established two different intuitive metrics for curvature:

$$curvature\ 1 = \frac{alpha\text{-}space}{pocket\ SA} \tag{1}$$

and

$$curvature\ 2 = \frac{desolvated\ alpha\text{-}cluster\ SA}{total\ alpha\text{-}cluster\ SA} \tag{2}$$

for two simple SA-based pocket metrics:

$$SA\ score\ 1 = curvature\ 1 \times (desolvated\ pocket\ SA + desolvated\ alpha\text{-}cluster\ SA) \tag{3}$$

and

$$SA\ score\ 2 = curvature\ 2 \times (desolvated\ pocket\ SA + desolvated\ alpha\text{-}cluster\ SA) \tag{4}$$

A model depicting the components used to calculate these SA-based scores can be visualized in Fig. S12. Pocket and alpha-cluster SAs are calculated using the open source software Naccess.[4]

In Fig. S13, the alpha-space of all PPI interface pockets is plotted against the various volume and structure-based pocket metrics we have described: atom-excluded alpha-space (discussed below), total desolvated SA, *SA score 1*, *SA score 2*, total alpha sphere volume, and total alpha-cluster volume. The remarkably high correlations between total alpha-space and both *SA score 1* ($r = 0.97$) and *SA score 2* ($r = 0.94$) support our original hypothesis that total alpha-space could be utilized as a strong proxy for a general curvature-weighted surface area metric. The near perfect correlation between total alpha-space

and atom-excluded alpha-space is interesting, however we ultimately choice to evaluate pockets using total alpha-space. While the atom-excluded alpha-space has a more physical meaning, our application of alpha-space in pocket scoring is designed to represent not a physical volume, but a more abstract metric of general binding potential. Furthermore, the association of alpha spheres with fractional alpha-spaces, rather than full alpha-spaces, could compromise the pocket occupation model discussed below. Similarly, the advantage of evaluating pockets with alpha-space over these explicit SA-based scores derives from the ability to easily subdivide a pocket into occupied and unoccupied spaces due to the discrete nature of the individual alpha sphere/space pairs.

Fig. S14 compares the enrichment at the 2P2I PPI and iPPI interfaces for high scoring pockets ranked according to three different criteria: pocket score, alpha-space volume, and ratio of nonpolar space:

$$ratio\ of nonpolar\ space = \frac{pocket\ score}{alpha\text{-}space} \tag{6}$$

All three pocket-ranking criteria result in PPI and iPPI interfaces significantly enriched with high-ranking pockets, but the highest enrichment is seen when ranking by the AlphaSpace pocket score. While the interfaces are technically un-enriched for low ranking alpha-clusters, it is notable that we detect many lower scoring pockets participating in both PPI and iPPI interfaces.

Section S5. Pocket-fragment complementarity

Early work by Jie Liang et al. introduced a pocket volume metric calculated by subtracting from a pocket's total alpha-space the portion overlapping with the VdW volume of the pocket atoms.[6] We refer to this volume metric, originally implemented in CAST, as the atom-excluded alpha-space. Intuitively, pocket-fragment complementarity—or "pocket occupation"—could be calculated from the physical overlap between the atom-excluded alpha space and the VdW volume of the peptide or inhibitor atoms bound to that pocket. While this metric is physically meaningful in deep pockets for which a binding fragment will physically occupy the atom-excluded alpha-space (see Fig. 3C), it loses this physical relevance for shallow pockets. Even the highly complementary alpha-cluster lies generally outside of a shallow pocket's alpha-space (see Fig. 3B) and would, as a theoretical fragment, falsely result in a zero or near-zero pocket occupation. Fig. S15 shows that, for many PPI pockets, there is, in fact, a near-zero physical overlap between interacting fragment atoms and the atom-excluded alpha-space.

Alternatively, AlphaSpace evaluates pocket occupation from the contact between alpha sphere centers and the interacting peptide/inhibitor atoms. From Fig. S15, we see a broad range of non-zero occupations is detected with this metric. From a design perspective, converting partially occupied pockets to fully occupied pockets will improve pocket-fragment complementarity and should augment inhibitor affinity by increasing the amount of inhibitor surface area to be desolvated in the formation of the binding complex and through the formation of additional VdW interactions due to tighter and more extensive interfacial atomic packing.

Section S6. Pocket volume

The "real volume" pocket feature used in fpocket is the union of the alpha sphere volumes for an alpha-cluster, calculated using the full alpha sphere radii (see Fig. S13E). Pocket volume by this metric is particularly misleading for the geometries of the shallow pockets found at PPIs. As the concave space represented by an alpha sphere gets flatter, its alpha sphere radius gets larger. This phenomenon results in large pocket volumes assigned to shallow pockets, for which much of the alpha sphere volume lies outside the meaningful interaction space. A more meaningful alpha-cluster volume can be calculated using the alpha-atoms, with 1.8 Å radii to represent generic nonpolar ligand atoms (see Fig. S13F). This alpha-cluster volume can be used to approximate the molecular volume of a pocket's complementary ligand fragment. Volumetric data presented in the Results section is approximated by randomly sampling 20,000 points within an enclosing box, calculating the ratio of points falling within the shape, and multiplying by the box volume.

Section S7. Additional pocket features

AlphaSpace can calculate a number of additional pocket features (see Tables S3). Pocket-centric features include: number of pocket atoms, number of polar pocket atoms, and whether or not a pocket contains a charged group. Peptide-centric features include: residue IDs of peptide side chains occupying a pocket, residue IDs of peptide backbone atoms occupying a pocket, number of peptide/ligand atoms occupying a pocket, number of polar peptide/ligand atoms occupying a pocket, and whether or not the pocket-occupying atoms include a charged group.

Section S8. Dataset details

In testing FCTM on the PPI/iPPI/Apo systems from the 2P2I dataset, we omitted two systems indexed in the database due to incompatibility with our comparative analysis. The HPV regulatory protein E2 complexes are omitted due to inconsistency in the sequences solved for the PPI and iPPI structures. The E2 in the PPI is the enhancer protein for HPV18 (PDB: 1tue), while the E2 in the iPPI is the enhancer for HPV11 (PDB: 1r6n). This sequence variation prohibits the direct atomistic comparison of the pockets. The TNFR1 complexes are omitted because the inhibitor in the iPPI structure is a covalently bound inhibitor (PDB: 1ft4), which lacks the type of non-covalent pocket-fragment interaction under investigation here. Additionally Mdm4, Xdm2, and Hpv-E2 have no apo structures available.

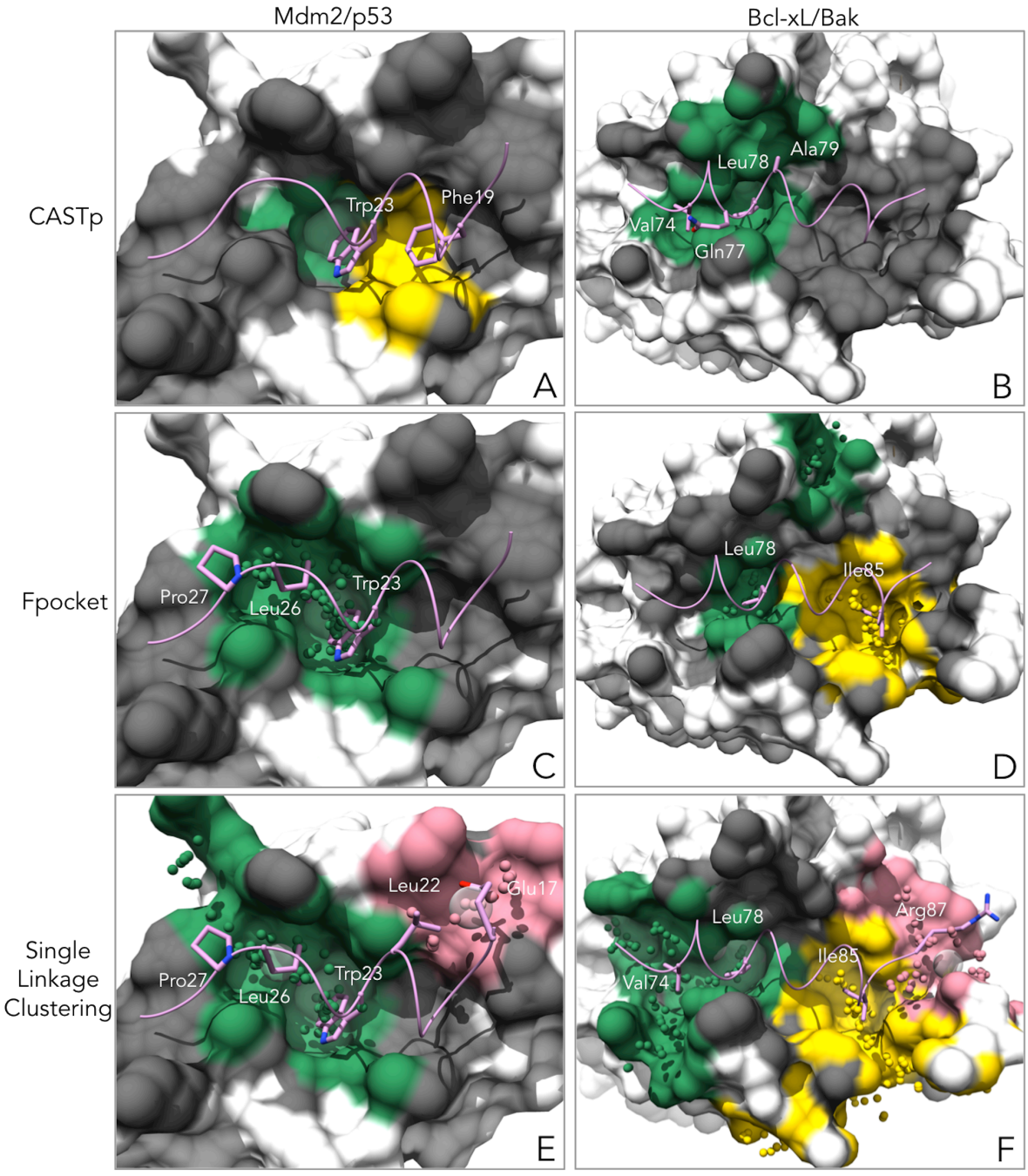

Figure S1. PPI interface pocket detection results for Mdm2/p53 (left) and Bcl-xL/Bak (right) using three existing geometry-based methods: CASTp[7] (top), fpocket[8] (center), single-linkage clustering similar to SiteFinder[9] (bottom). Green, yellow, and pink represent individual pockets, and the grey surface indicates the full PPI interface, defined as any surface atom with reduced SASA upon placement of the peptide, calculated using Naccess.[4] Comprehensive coverage of the interface is generally not observed. Pocket definitions are inconsistent between methods and tend to extend beyond local fragment-centric interactions (as in B, C, E, and F) or into the solvent-inaccessible interior of the protein (as in D).

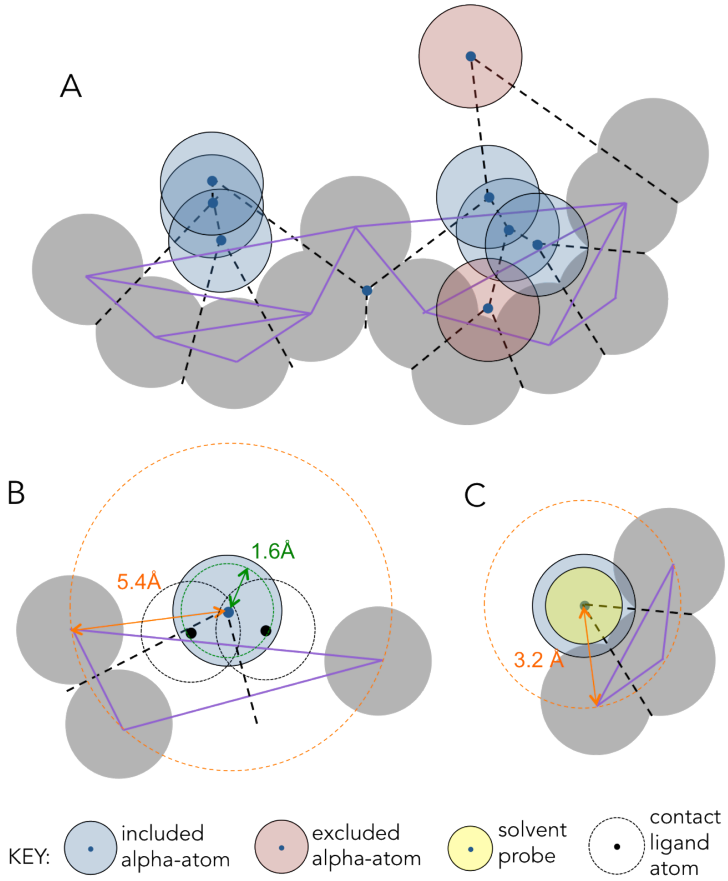

Figure S2. (A) 2-dimensional schematic of two fragment-centric pockets in a protein surface, depicting the alpha-atom/alpha-space model. Dashed lines represent edges from the Voronoi tessellation; the Delaunay triangulation, in purple, forms the contiguous alpha-space area. Blue circles represent alpha-atoms included in the topographical mapping (radius is 3.2-5.4 Å); red circles are alpha-atoms to be filtered out by radius. Alpha-atoms are assigned a 1.8 Å radius to emulate theoretical nonpolar ligand atoms. (B) Alpha-system—alpha sphere (orange), alpha-atom (blue), and alpha-space (purple)—at maximum radius cutoff (5.4 Å). Example "contact" ligand atoms (black outline) serve to illustrate the geometric relationship between the protein surface and atoms at the contact distance limit (1.6 Å). (C) Alpha-system at minimum radius cutoff (3.2 Å). A superimposed 1.4 Å solvent probe (yellow) illustrates that this is the solvent-accessibility limit for intraction space represented by an alpha sphere.

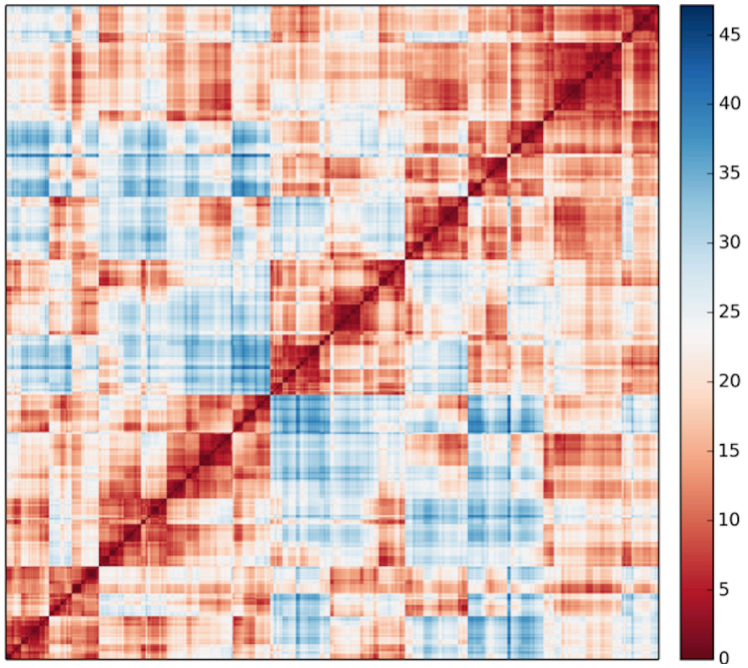

Figure S3. Dendrogram for an average-linkage hierarchical clustering of alpha spheres at the surface of Mdm2 (PDB: 1ycr) based on Euclidian distance (Å). Cells in the matrix are colored according to a 3-color gradient to reflect each pairwise alpha sphere distance (red: d = 0 Å, white: d = 22.5 Å, blue: d = 50 Å).

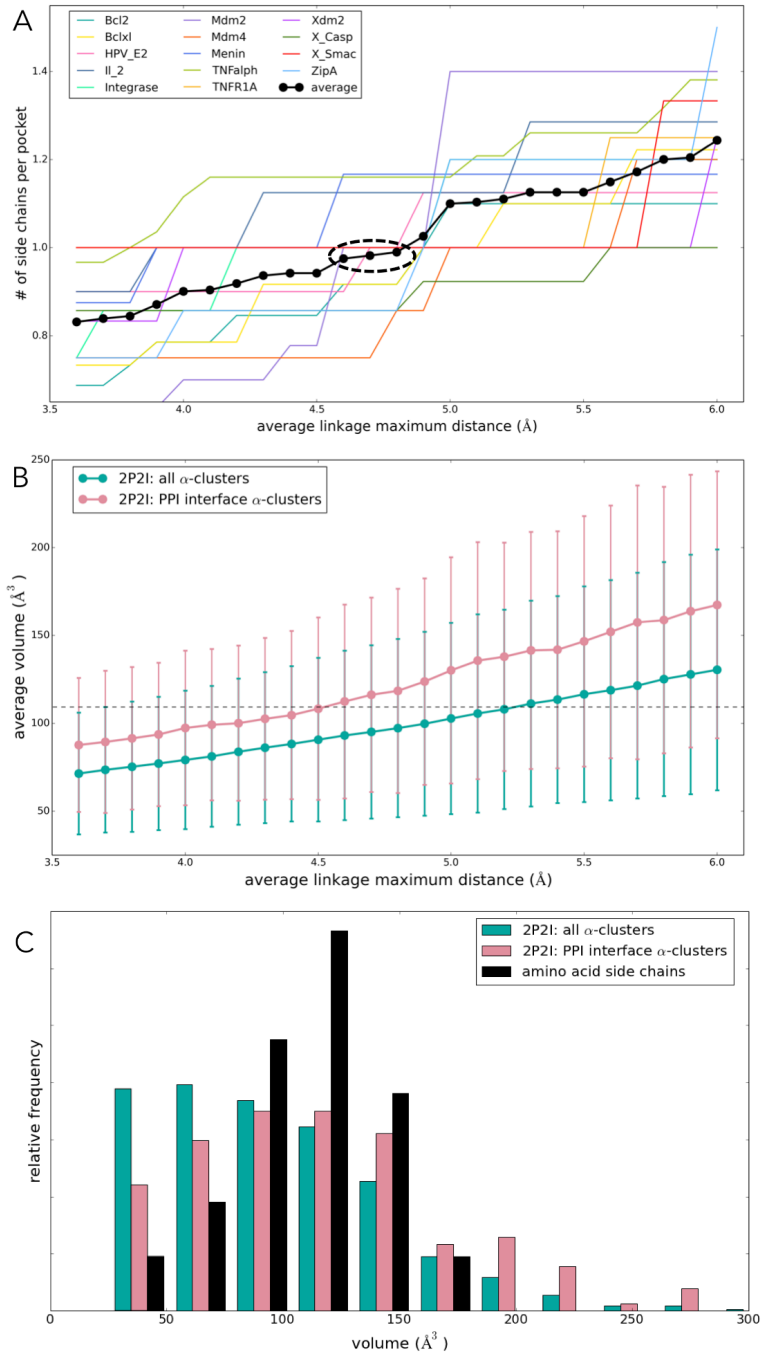

Figure S4. (A) The number of interacting peptide side chains per pocket as a function of the average linkage maximum distance for the 14 PPI interfaces in the 2P2I. The average number of side chains per pocket is near unity from 4.6-4.8 Å, indicating a promising range for fragment-centric clustering. (B) Average and standard deviation of alpha-cluster volume as a function of average linkage maximum distance for the complete set of alpha-clusters (teal) and for the subset of interface alpha-clusters (pink). The black dashed line marks 109.2 Å, the average volume of the 20 natural amino acids. (C) Normalized histograms of the alpha-cluster volumes using the 4.7 Å average linkage maximum distance, overlaid with the histogram of amino acid volumes, for reference.

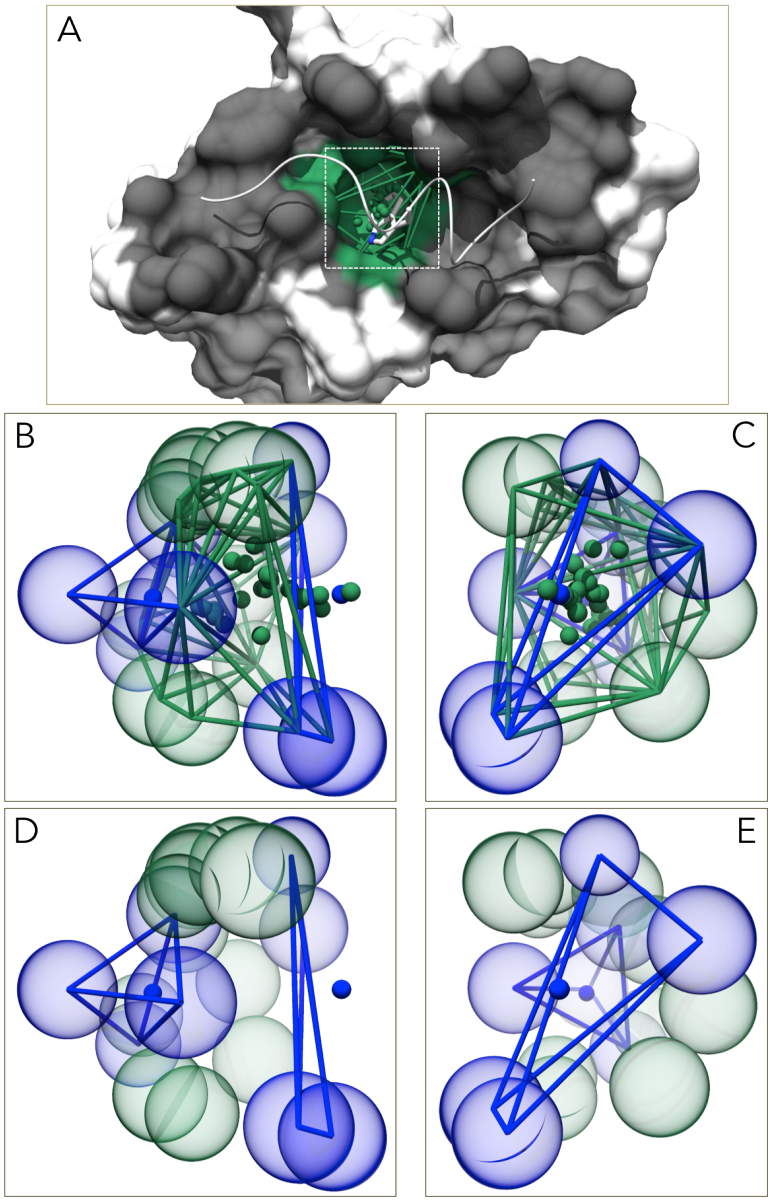

Figure S5. Pocket-lining atoms, alpha sphere centers, and alpha-spaces for the Mdm2/p53 Trp92 pocket. (A) Shown in the context of the protein surface (PDB: 1ycr). (B, C) The entire alpha-cluster is shown (small green spheres) with two selected alpha spheres (small blue spheres) and their respective pocket-atoms (large transparent green and blue spheres) and alpha-spaces (green and blue tetrahedron). (B) side-view, (C) birds-eye view of the pocket. (D, E) Displaying only the blue alpha spheres and alpha-spaces for a clearer visualization of the alpha sphere/alpha-space relationship, all pocket-atoms remain displayed as transparent green and blue spheres.

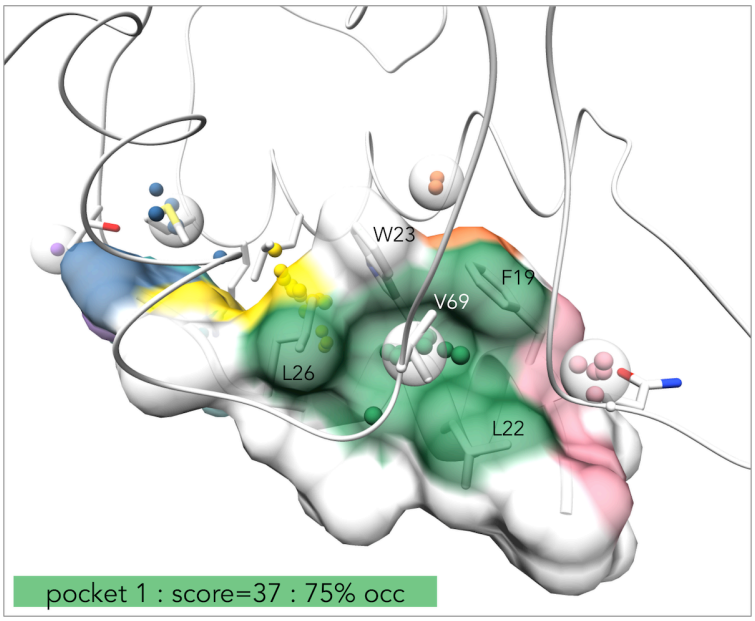

Figure S6. Mapping of the p53 surface of the Mdm2/p53 interface, highlighting pocket 1, formed by the three p53 hot spot residues (W23, F19, L26) and L22. The role of L22 in the formation of this pocket, which binds V69 from Mdm2, may account for the residue's significant contribution to Mdm2/p53 affinity despite the low scoring pocket from Mdm2 to which it binds.

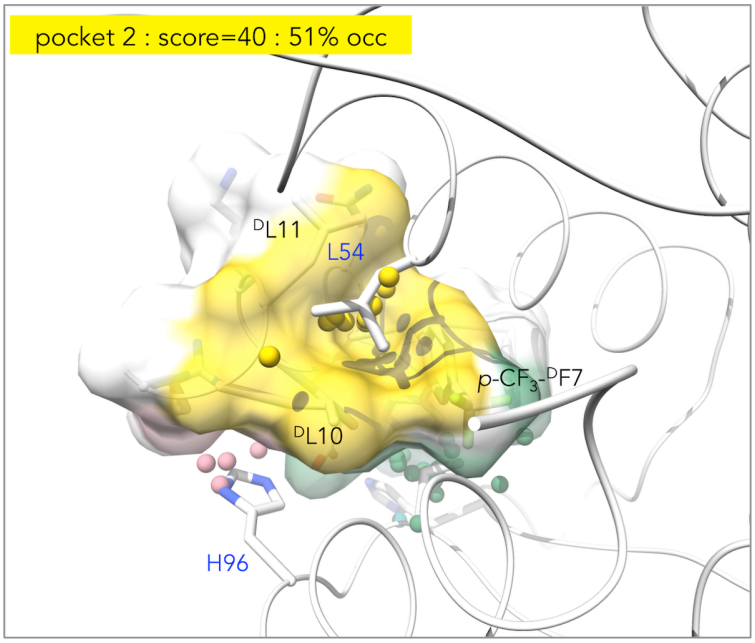

Figure S7. Mapping of the $_{D}$-peptide antagonist surface of the Mdm2/^{D}PMI-δ interface, highlighting pocket 2, formed by ^{D}L11, *p*-CF_3-^{D}F7, and ^{D}L10. The role of ^{D}L10 in the formation of this pocket, which binds L54 from Mdm2, may account for the residue's contribution to Mdm2/^{D}PMI-δ affinity despite the low scoring pocket from Mdm2 to which it binds. Black residue labels are the $_{D}$-peptide; blue labels are Mdm2.

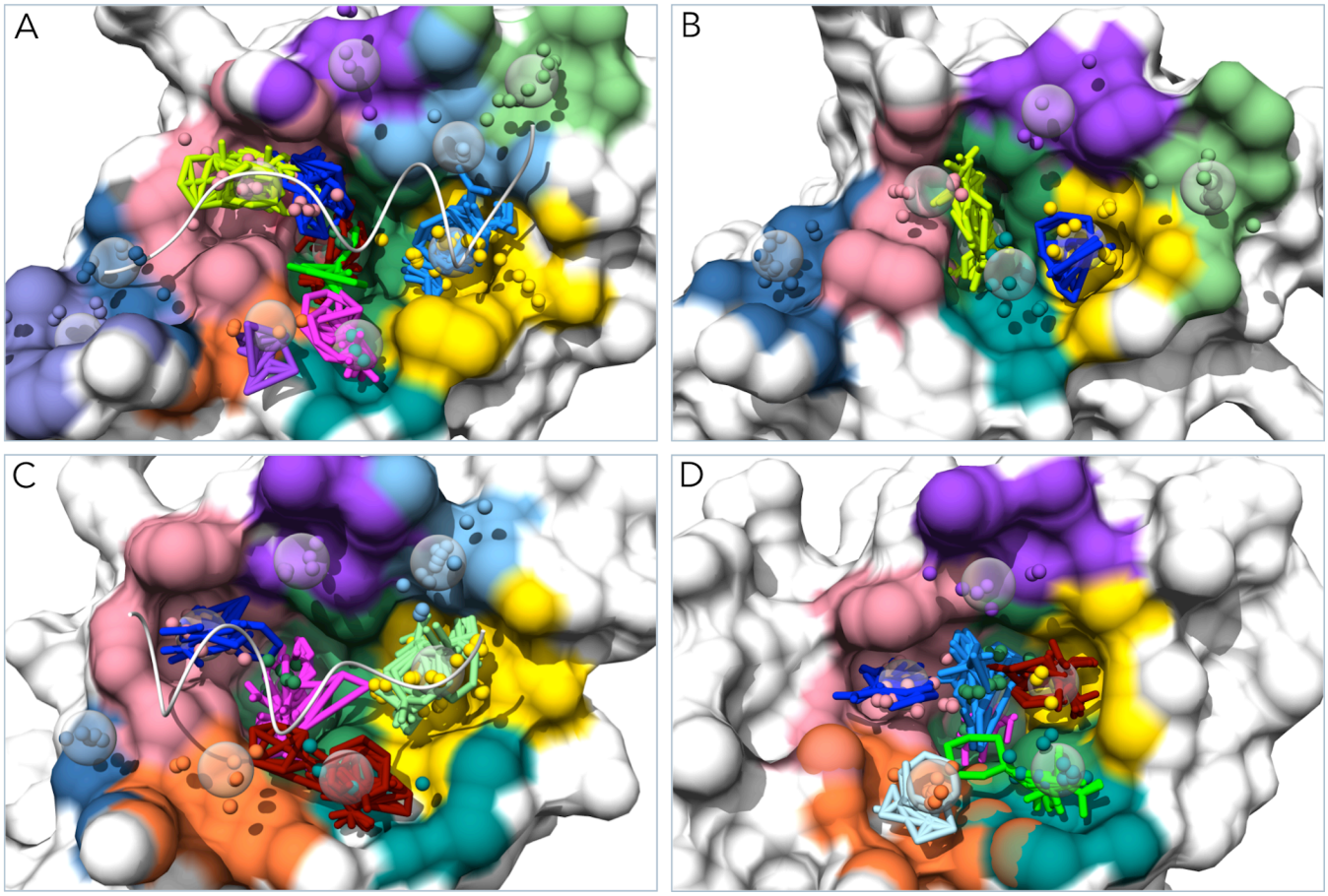

Figure S8. Comparing FTMap results and AlphaSpace results for the Mdm2 interfaces: (A) Mdm2/p53, (B) Apo, (C) Mdm2/^{D}PMI-δ (D) Mdm2/ small molecule inhibitor. Probe clusters from FTMap are represented as sticks, alpha-centers from AlphaSpace are represented as spheres. p53 peptide and ^{D}PMI-δ are included for reference (white).

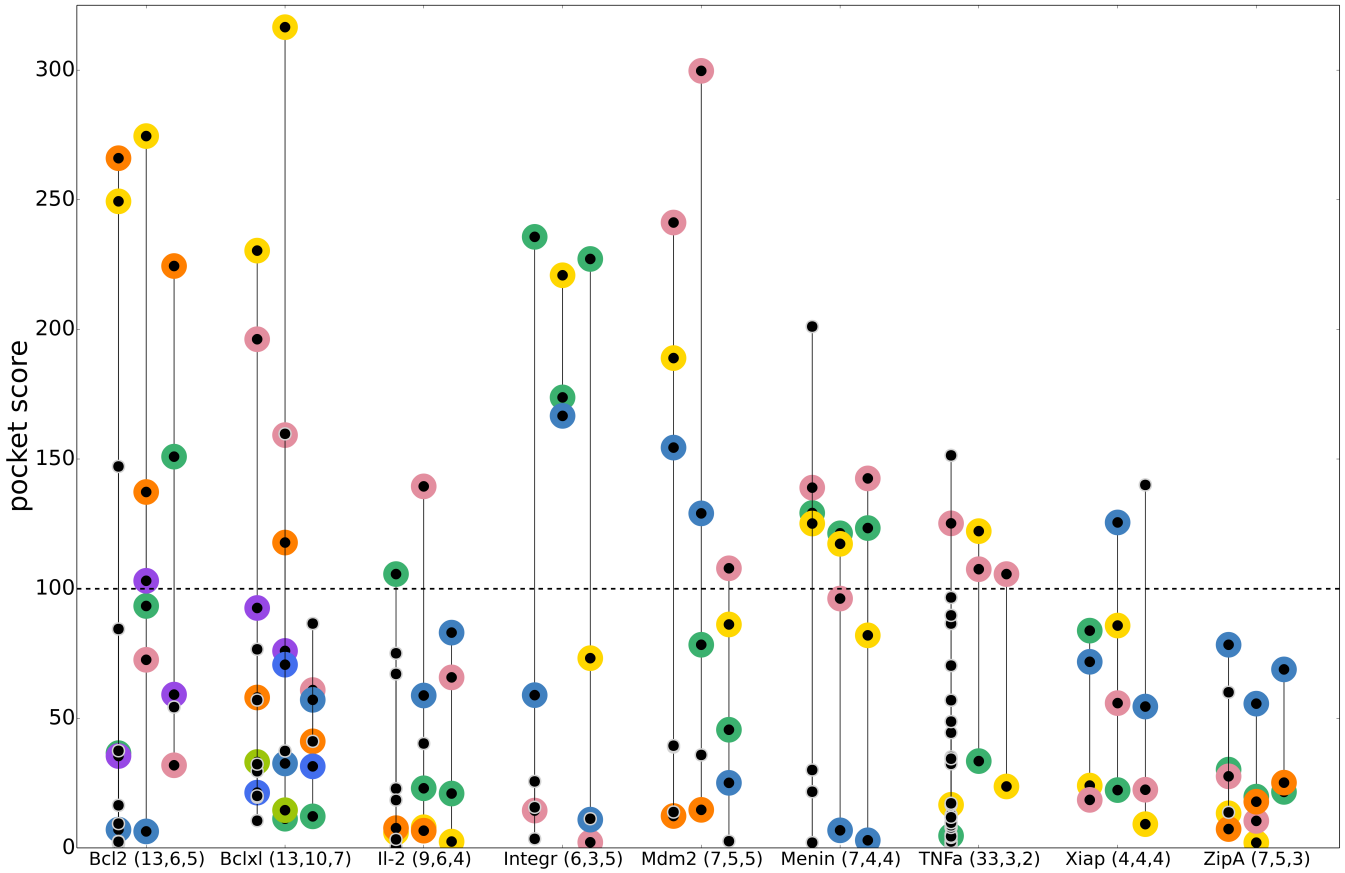

Figure S9. *Pocket matching* between PPI interfaces, iPPI interfaces, and apo protein surfaces. Each fragment-centric interface pocket is represented by a black circle along the pocket score axis (PPI: left, iPPI: center, Apo: right). Matching pockets are designated with color-coordinated rings between each PPI/iPPI/Apo set. The total interface pocket counts for each system are listed in parentheses for PPI, iPPI, and Apo respectively.

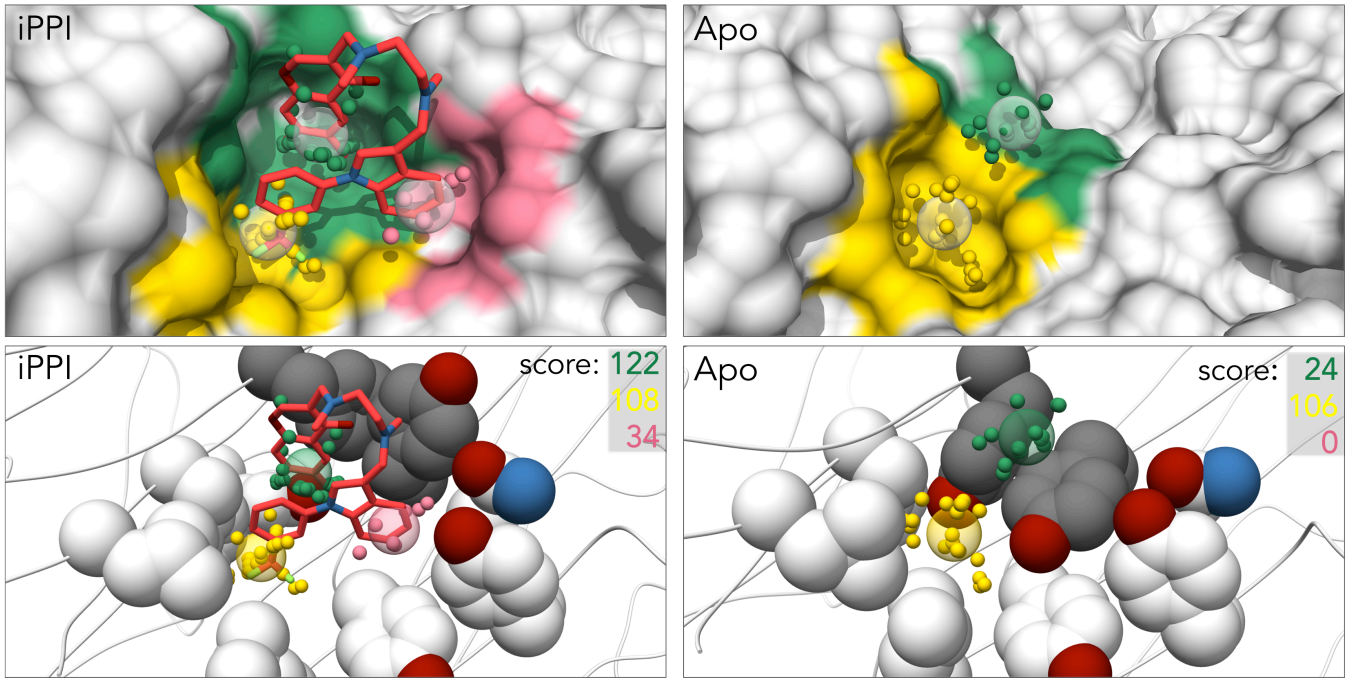

Figure S10. Example of pocket modulation at the fragment-centric resolution. For TNF-alpha, between the iPPI and the Apo state structures, one fragment-centric pocket is attenuated (green, score 122 to 24), one disappears (pink, score 34 to 0), and the third pocket goes essentially unchanged (yellow, score 108 to 106).

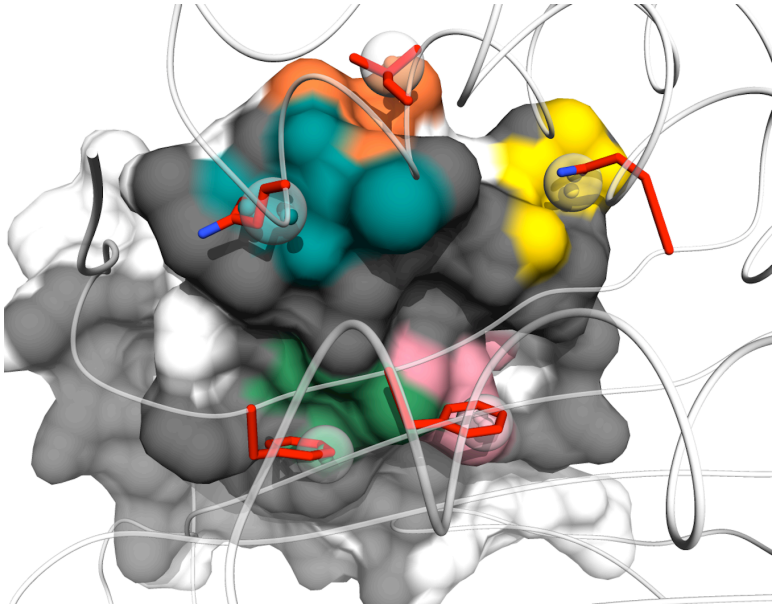

Figure S11. Xiap-Bir3/Caspase-9 interface highlighting well-defined fragment-centric modularity for small pockets defined by only 1 or 2 alpha spheres.

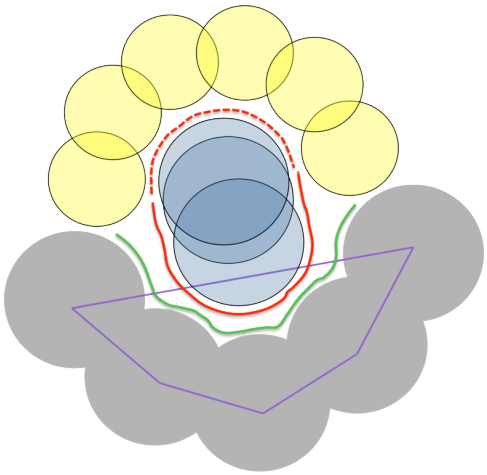

Figure S12. Schematic depicting the components used for the SA-based and alpha-space-based scoring metrics: pocket-atoms in surface representation (grey), alpha-cluster (blue), and solvent probes (yellow), SA of the pocket desolvated by the alpha-cluster (green), SA of the alpha-cluster desolvated by the pocket (solid red), SA of the alpha-cluster still solvated in the complex (dashed red), and total alpha-space (purple).

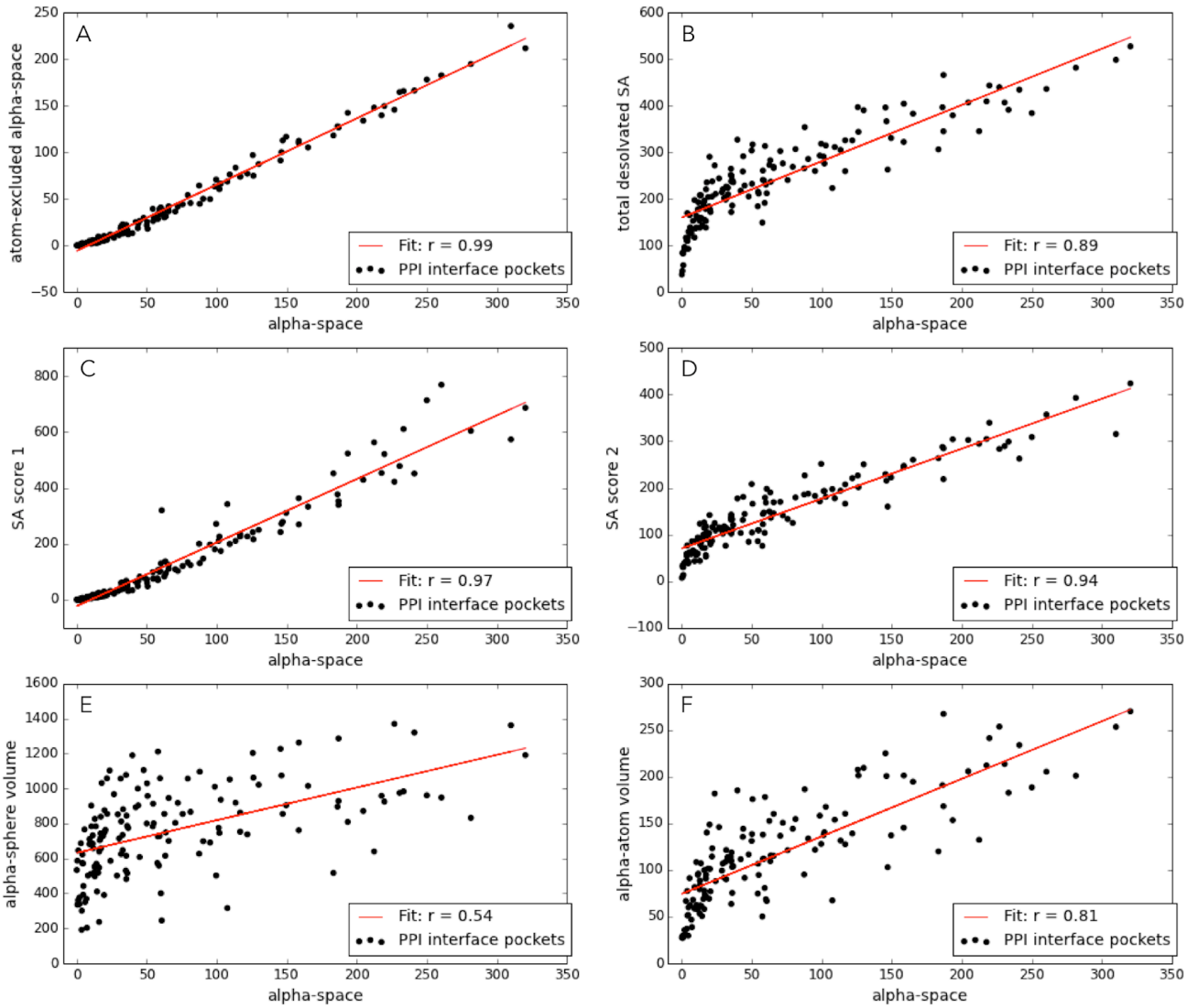

Figure S13. Correlations of alpha-space with various pocket features for all interface pockets from the 14 2P2I PPI complexes (black), linear fit (red). (A) Atom-excluded alpha-space: r = 0.99, (B) Total desolvated surface area for the alpha-cluster/pocket complex: r = 0.89, (C) *SA score 1*: r = 0.97, (D) *SA score 2*: r = 0.94, (E) the union alpha sphere volume (equivalent to fpocket's "real volume" descriptor): r = 0.54, (F) the union alpha-atom volume (or the alpha-cluster volume): r = 0.81.

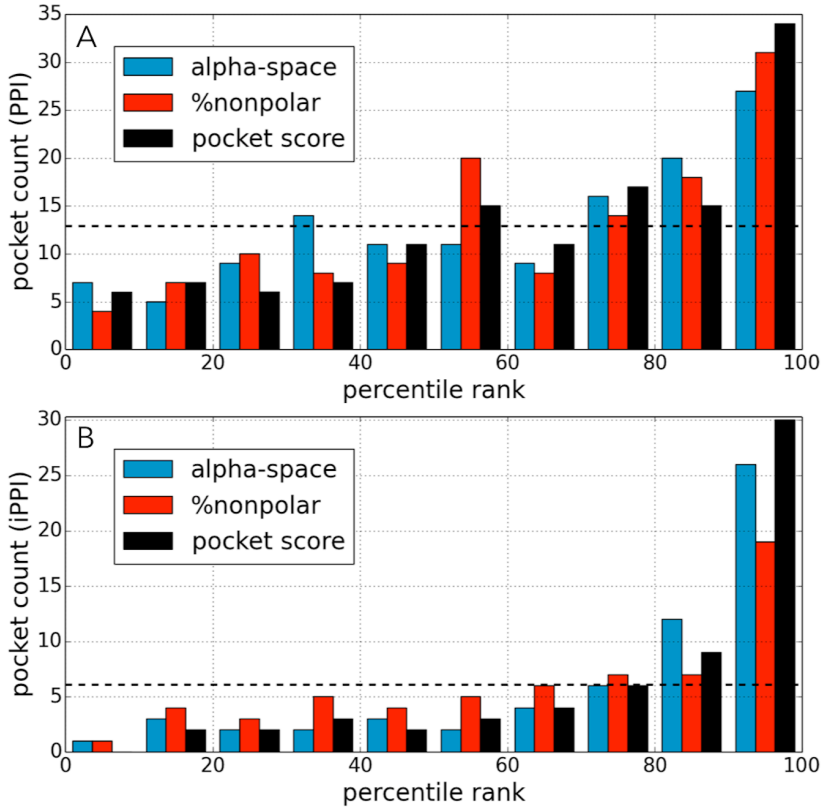

Figure S14. Histograms illustrating the distributions for the percentile rankings of all interface pockets taken from the 2P2I database: (A) PPIs, (B) iPPIs. Ranking is calculated based on alpha-space (blue), non-polarity (red), and pocket score (black). Dashed black lines represent the statistically expected, uniform distributions.

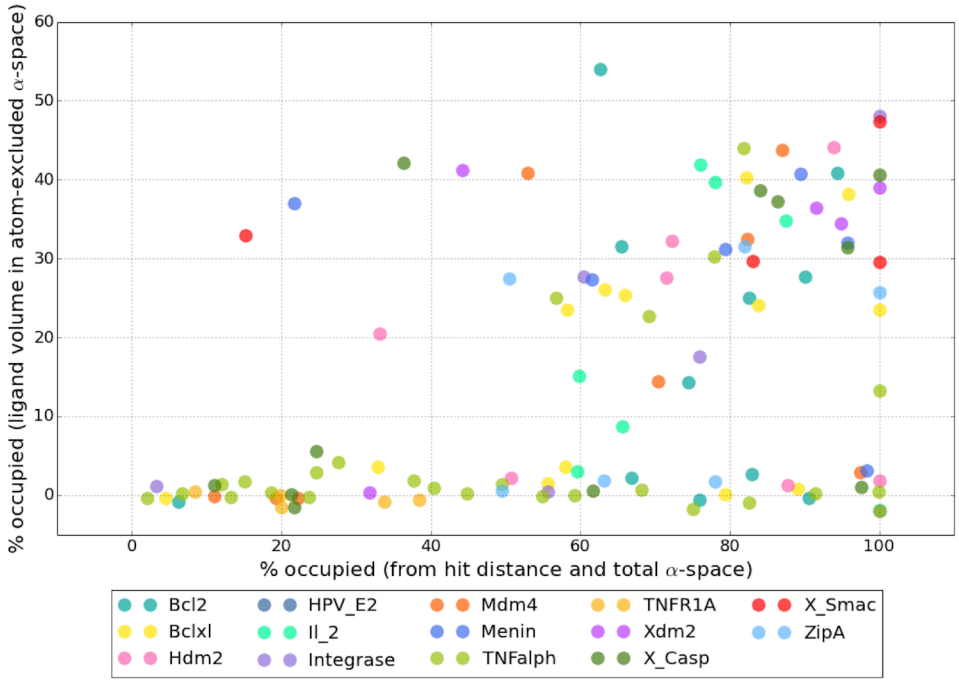

Figure S15. Two different pocket occupation metrics are compared for the complete set of PPI interface pockets from the 14 proteins in the 2P2I database. X-axis: the sum of the alpha-space volumes associated with alpha spheres in contact with peptide atoms divided by the total alpha-space. Y-axis: the fraction of the atom-excluded alpha-space that is physically occupied by the VdW volume of peptide atoms.

rank	color	score	% occupied	alpha-space	%non-polar
1	green	264	46%	265	100%
2	yellow	185	16%	206	90%
3	pink	70	61%	132	53%
4	teal	65	92%	68	96%
5	orange	48	51%	93	52%
6	blue	46	38%	64	72%
7	purple	45	65%	60	75%
8	ltblue	36	80%	43	84%
9	peri	33	38%	51	65%
10	peach	15	26%	46	33%
11	tan	12	44%	24	50%

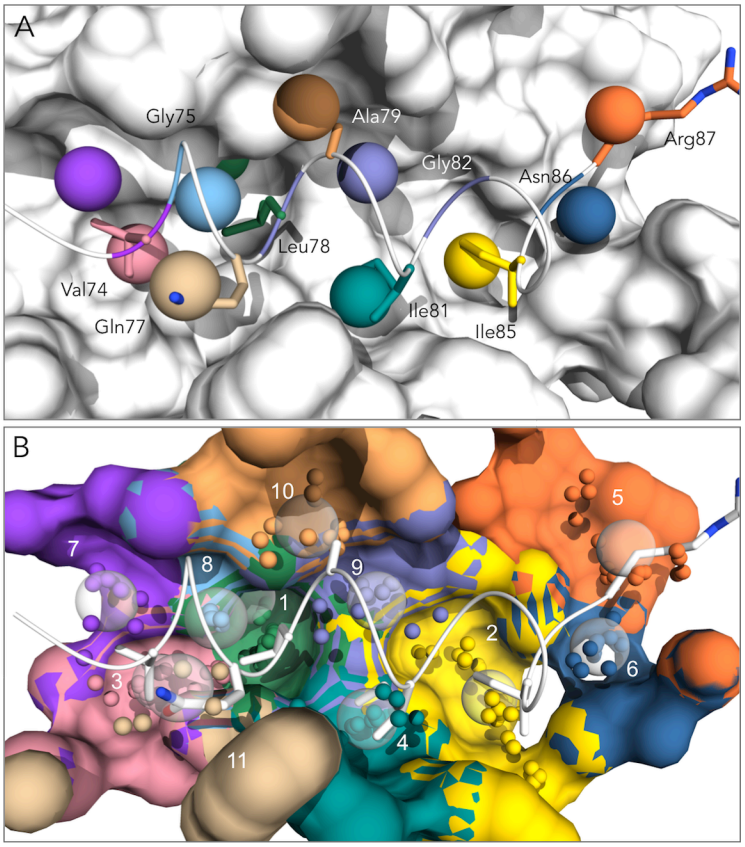

Figure S16. Alpha-space-based pocket features are presented for the 11 contact pockets at the Bcl-xL/Bak PPI interface. (A, B) Different visual representations of the FCTM result for Bcl-xL/Bak. (A) Interface pockets are represented by the centroid of each alpha-cluster. The side chains from Bak are displayed and labeled whenever they make contact with one of the interface pockets, and pocket-fragment interactions are color-coordinated. Peptide backbone fragments are represented in color on the coil. The natural modularity of the surface is exhibited in the overlap between the centroids and the side chains. (B) Each pocket is represented as a surface, alpha sphere centers are shown as small spheres colored by pocket, and the alpha-cluster centroids are depicted as large transparent spheres. Pockets are numbered by rank, as in the table.

Table S1. PDB-ID list for all PPI/iPPI structures used from the 2P2I database[2]

System (2P2I)	PPI (PDB-ID)	iPPI (PDB-ID)	Apo (PDB-ID)
Bcl2/Bax	2XA0	4AQ3	1GJH
Bcl-xL/Bad	2BZW	2YXJ	1R2D
Hpv-E2/Hpv-E1	1TUE	1R6N	
Il-2/Il-2R	1Z92	1PY2	1M47
Integrase/LEDGF	2B4J	4E1N	1BI4
Mdm2/p53	1YCR	4ERF	1Z1M
Mdm4/p53	3DAB	3LBJ	
Menin/MLL	4GQ6	4GQ4	4GPQ
TNFalpha/TNFalpha	1TNF	2AZ5	3L9J
TNFR1-A/TNFR1-B	1TNR		
Xdm2/p53	1YCQ	1TTV	
Xiap/Caspase	1NW9		
Xiap/Smac	1G73	2JK7	1F9X
ZipA/FtsZ	1F47	1Y2F	1F46

Table S2. Experimental alanine scanning results for Mdm2/p53,[10] calculated from K_d values. $\Delta\Delta G > 3.0$ kcal/mol (red), $2.0 < \Delta\Delta G < 3.0$ kcal/mol (blue). "n.d." indicates a binding affinity below the detectable limit.

	Mdm2/p53	
ala mut	**K_d(μM)**	**ΔΔG (kcal/mol)**
WT	0.44	0
Glu17	0.56	0.1
Thr18	1.2	0.6
Phe19	n.d.	n.d.
Ser20	0.21	-0.4
Asp21	0.83	0.4
Leu22	5.0	1.4
Trp23	n.d.	n.d.
Lys24	0.23	-0.4
Leu25	0.73	0.3
Leu26	27	2.4
Pro27	0.051	-1.3
Glu28	0.24	-0.4

Table S3. Pocket-centric and peptide-centric features of the Mdm2/p53 interface pockets. (See Section S7 for descriptions.)

rank	color	# pocket atoms	polar pocket atoms	charged group	peptide side chain resIDs	peptide backbone resIDs	# peptide atoms	polar peptide atoms	peptide charged group
1	green	19	3	no	23		7	0	no
2	yellow	20	4	no	19,23	19,20,23	13	2	no
3	pink	22	4	no	26,27	26,27	8	2	no
4	teal	15	5	yes	29		3	2	no
5	orange	12	4	yes	29	28,29	10	4	no
6	blue	12	7	yes	17		5	2	yes
7	purple	9	2	no	22		3	0	no

Table S4. Total interface surface areas for PPIs and iPPIs and the percentage of the interface surface areas covered by each set of fragment-centric contact pockets identified by AlphaSpace.

	PPI		iPPI	
system	interface surface area (Å^3)	% interface coverage by AlphaSpace	interface surface area (Å^3)	% interface coverage by AlphaSpace
Bcl-2	1031	95	478	97
Bcl-xL	1008	92	530	100
HPV-E2	909	80	275	88
Il-2	937	80	387	97
Integrase	589	78	280	100
Mdm2	660	92	292	100
Mdm4	529	90	358	86
Menin	709	96	253	95
TNFalpha	2228	89	266	88
TNFR1A	633	77		
Xdm2	462	94	307	99
Xiap-Casp	998	91		
Xiap-Smc	255	93	278	97
ZipA	544	94	243	97

Table S5. Experimental alanine scanning results for Bcl-xL/Bak,[11] calculated from K_d values. $\Delta\Delta G > 3.0$ kcal/mol (red), $2.0 < \Delta\Delta G < 3.0$ kcal/mol (blue). "n/a" indicates that the mutagenesis was not performed.

	Bcl-xL/Bak	
ala mut	**K_d(μM)**	**ΔΔG (kcal/mol)**
WT	0.34	0
Val74	15	2.2
Gly75	n/a	n/a
Arg76	3.3	1.3
Gln77	n/a	n/a
Leu78	270	3.9
Ala79	0.34	0.0
Ile80	1.0	0.6
Ile81	17	2.3
Gly82	0.50	0.2
Asp83	41	2.8
Asp84	0.14	-0.5
Ile85	93	3.3

Table S6. Pocket-centric and peptide-centric features of the Bcl-xL/Bak interface pockets

rank	**color**	**# pocket atoms**	**polar pocket atoms**	**charged group**	**peptide side chain resIDs**	**peptide backbone resIDs**	**# peptide atoms**	**polar peptide atoms**	**peptide charged group**
1	green	24	4	no	78		4	0	no
2	yellow	27	9	yes	85		4	0	no
3	pink	16	2	no	74,78		3	0	no
4	teal	16	3	no	81	81	6	1	no
5	orange	14	5	no	87	87	5	1	no
6	blue	12	6	no	87	85,86,87	5	3	no
7	purple	12	4	yes		74	4	2	no
8	ltblue	6	1	no		75	3	1	no
9	peri	15	3	yes		78,82	4	1	no
10	peach	15	7	yes	79	75,79	3	1	no
11	tan	10	2	no	77	77	5	1	no

REFERENCES

(1) Bourgeas, R.; Basse, M.-J.; Morelli, X.; Roche, P. Atomic Analysis of Protein-Protein Interfaces with Known Inhibitors: The 2P2I Database. *PLoS One* **2010**, *5*, e9598.

(2) Basse, M. J.; Betzi, S.; Bourgeas, R.; Bouzidi, S.; Chetrit, B.; Hamon, V.; Morelli, X.; Roche, P. 2P2Idb: A Structural Database Dedicated to Orthosteric Modulation of Protein-Protein Interactions. *Nucleic Acids Res.* **2013**, *41*, D824–D827.

(3) Darby, N. J.; Creighton, T. E. Protein Structure; IRL Press at Oxford University Press, 1993; p 99.

(4) Hubbard, S. J.; Thornton, J. M. NACCESS, Computer Program, Department of Biochemistry and Molecular Biology, University College London, 1993.

(5) Cheng, A. C.; Coleman, R. G.; Smyth, K. T.; Cao, Q.; Soulard, P.; Caffrey, D. R.; Salzberg, A. C.; Huang, E. S. Structure-Based Maximal Affinity Model Predicts Small-Molecule Druggability. *Nat. Biotechnol.* **2007**, *25*, 71–75.

(6) Liang, J.; Edelsbrunner, H.; Woodward, C. Anatomy of Protein Pockets and Cavities: Measurement of Binding Site Geometry and Implications for Ligand Design. *Protein Sci.* **1998**, *7*, 1884–1897.

(7) Binkowski, T. A.; Naghibzadeh, S.; Liang, J. CASTp: Computed Atlas of Surface Topography of Proteins. *Nucleic Acids Res.* **2003**, *31*, 3352–3355.

(8) Le Guilloux, V.; Schmidtke, P.; Tuffery, P. Fpocket: An Open Source Platform for Ligand Pocket Detection. *BMC Bioinformatics* **2009**, *10*, 168.

(9) Molecular Operating Environment (MOE), 2013.08; Chemical Computing Group Inc., 1010 Sherbooke St. West, Suite #910, Montreal, QC, Canada, H3A 2R7, 2014.

(10) Li, C.; Pazgier, M.; Li, C.; Yuan, W.; Liu, M.; Wei, G.; Lu, W.-Y.; Lu, W. Systematic Mutational Analysis of Peptide Inhibition of the p53-MDM2/MDMX Interactions. *J. Mol. Biol.* **2010**, *398*, 200–213.

(11) Sattler, M. Structure of Bcl-xL-Bak Peptide Complex: Recognition Between Regulators of Apoptosis. *Science (80-.).* **1997**, *275*, 983–986.